scientific reports

OPEN

The impact of biodegradable plastics on methane and carbon dioxide emissions in soil ecosystems: a Fourier transform infrared spectroscopy approach

Yihao Wang[1,2], Leizi Jiao[1], Chunjiang Zhao[1], Wentao Dong[1], Wenwen Gong[1✉] & Daming Dong[1✉]

Biodegradable plastics (BPs), promising eco-friendliness, raise environmental concerns as they degrade into numerous microplastics (Bio-MPs). The impact of Bio-MPs on methane (CH_4) and carbon dioxide (CO_2) emissions in soil ecosystems remains largely unexplored. Utilizing Fourier transform infrared (FTIR) spectroscopy, we innovatively designed a circulating system, integrating a long optical-path gas cell with a static chamber for continuous and convenient CH_4/CO_2 monitoring in paddy soils with the addition of Bio-MPs (PBAT). On the 7th day of incubation, we observed a significant increase in CH_4/CO_2 absorption peaks due to the addition of PBAT, with enhancements of 92-fold and 213-fold, respectively. Built upon this system, we explored a quantitative method based on the main absorption peak (3010 cm^{-1}) for CH_4, and calculated cumulative emissions. Additionally, we analyzed attenuated total reflection (ATR) spectra of soil with and without Bio-MPs based on FTIR spectrometer, revealing the characteristic response in soil ATR spectra triggered by PBAT, and demonstrating ATR spectroscopy's potential for identifying soil contamination by Bio-MPs. This study aims to broaden and improve the utilization of FTIR spectroscopy for the purpose of monitoring soil GHG emissions and identifying soil contaminated by Bio-MPs, thereby offering significant insights into the influence of Bio-MPs on climate change.

Farmland, a crucial part of the terrestrial ecosystem, is a significant source of greenhouse gas (GHG) emissions[1]. The Intergovernmental Panel on Climate Change's 2019 report indicates that agriculture, forestry, and other land-use activities account for 23% of net anthropogenic GHGs[2]. Paddy fields are agricultural land specifically used for rice cultivation, typically located in low-lying areas with the ability to retain moisture. The flooded conditions required for rice cultivation significantly contribute to GHG emissions, particularly methane (CH_4), as the anaerobic environment enhances the activity of methanogens in the soil[1]. Plastic pollution, particularly microplastics (MPs, < 5 mm), has drawn significant attention due to its environmental impact and potential hazards[3,4]. As eco-friendly alternatives, biodegradable plastics (BPs) are being developed with better environmental acceptability and mechanical properties[5]. The degradability of biodegradable MPs is typically tested under conditions of high temperature and high humidity; hence their actual degradation ability in natural environments requires further study. Existing research primarily focuses on laboratory conditions and lacks long-term data on their behavior in the natural world[6]. However, soil GHG emissions are influenced by a variety of factors, including moisture, temperature, irrigation conditions, etc, there is a research gap in understanding the impact of these plastics, especially those that break down into Bio-MPs, on GHG emissions from farmland ecosystems[7,8]. This transition highlights the importance of investigating the influence of Bio-MPs on soil GHG emissions, which has not been extensively explored.

Currently, gas chromatography (GC) is widely used for monitoring GHGs from farmland[9-11]. However, the instrument is costly, operationally complex, and requires numerous auxiliary materials, including carrier gas and standard samples[12]. Fourier transform infrared (FTIR) spectroscopy is recognized as an accurate and fast technique for analyzing multiple gas components[13]. In the past ten years, our team has conducted research based on FTIR spectroscopy to identify volatile compounds during the food maturation and deterioration

[1]Beijing Academy of Agriculture and Forestry Sciences, Beijing 100097, China. [2]School of Agricultural Engineering, Jiangsu University, Zhenjiang 212013, China. ✉email: gong_ww@126.com; damingdong@hotmail.com

processes and detect soil nutrients, among other areas[14,15]. However, this traditional method often requires preparing multiple sets of samples or conducting multiple spectral collections on a single sample, involving repeated operations such as ventilating and collecting background spectra, which are labor-intensive and time-consuming[16]. Recently, we've combined a static chamber, commonly used for in-situ gas sampling in fields, with an FTIR spectrometer featuring a long optical-path gas cell, enabling cyclic gas measurement. We analyzed the collected spectral data to identify the absorption peaks of the target gas and determined the emission rate of the target gas based on the increment of absorbance per unit time. By simultaneously collecting gas samples for gas chromatography testing and performing correlation analysis, we were able to validate the accuracy of the results. This approach allows for continuous monitoring of soil CH_4 and carbon dioxide (CO_2) emissions, avoiding the operational complexities and inaccuracies of traditional extraction-based measurement methods.

Determining whether soil is contaminated with MPs can guide environmental protection efforts. While thermal analysis and Raman spectroscopy are commonly used methods, they also have their shortcomings, such as being destructive or having issues with fluorescence interference[17,18]. Attenuated total reflection (ATR) spectroscopy is an infrared spectroscopic technique that requires no complex sample preparation and applies to the analysis of solids, liquids, and viscous materials, particularly highlighting the identification of molecular structures in the surface or near-surface areas[19,20]. We investigated the ATR-FTIR spectroscopy of soil samples by fitting a spectrometer with an ATR accessory.

Herein, we aim to (1) employ long optical-path FTIR spectroscopy for continuous monitoring of CH_4/CO_2 emissions from typical paddy soils with the addition of Bio-MPs (PBAT); (2) develop and explore a quantitative method for CH_4 monitoring based on FTIR spectroscopy; (3) analyze the ATR-FTIR spectra of soil after Bio-MPs pollution. The outcomes of this study may refine the use of FTIR spectroscopy in monitoring soil GHG emissions and detecting soil contamination caused by Bio-MPs, and thereby contribute to advancing the understanding of impact of the Bio-MPs on the GHG dynamics in soil ecosystems.

Materials and methods
Materials
Paddy soil samples were collected from a rice field near Yanqing District, Beijing, China (40°27′28.93″N, 116°04′13.10″E) in December 2023 (Fig. 1a). According to information from local farmers, neither of the fields had previously used plastic mulches, and no other sources of microplastics (MPs) were identified. The soil samples had no significant microplastic contamination through the naked eye and microscope before the cultivation experiment, minimizing the impact of native MPs on the incubation experiments. The paddy soil with overlying water was collected from a depth of 0–20 cm, with around 10 sampling points randomly distributed across the entire field. After briefly removing roots, residues, and stones, the soil was placed in stainless steel containers and transported back to the laboratory at ambient temperature.

Presently, the most popular BPs in the market is Polybutylene adipate-co-terephthalate (PBAT), which accounts for 29.9% of global BPs production capacity[21]. Therefore, we have chosen it as a typical BPs. The PBAT
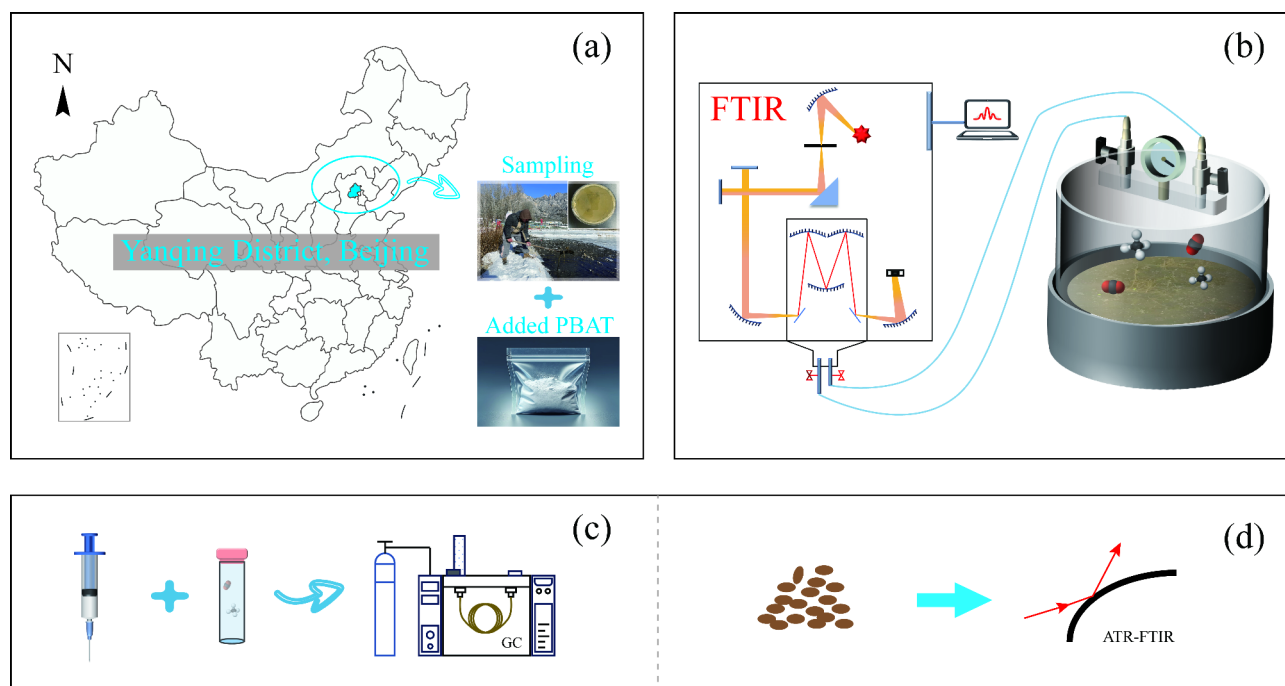

Fig. 1. Schematic diagram of experimental setup. (**a**) Sampling locations and cultivation of paddy soils. (**b**) Continuous monitoring of CH_4/CO_2 using long optical-path FTIR spectroscopy. (**c**) Measuring Gas Samples with GC. (**d**) Measuring the ATR spectra of Dried Soil Samples.

was obtained in powder form from Shanghai Guanbu ET Co., Ltd. (Shanghai, China). The powders used for the incubation experiments were homogenized in a mortar and sieved using a double-layer sieve to achieve a consistent size range of 75–150 μm, as previously described[22]. PBAT is a flexible, biodegradable polymer with a melting point of 110–120 °C and a density of 1.23 g/cm³. It has moderate oil and solvent resistance, good flexibility, thermal stability, and some chemical resistance, with mechanical strength generally lower than that of conventional plastics, and it is fully degradable in the natural environment[21].

Experimental design and sampling

Incubation experiments were conducted in a controlled environment chamber at a stable temperature of 25±1°C. All the collected soil samples were thoroughly mixed, and roughly 1 kg of paddy soil was positioned in a custom-designed glass cylinder (25 cm in diameter, 10 cm tall), topped with a 2 cm layer of water to ensure a flooded state during the incubation, with daily checks conducted. The experimental group, denoted as P-PBAT, involved blending PBAT into the paddy soil at a 1% (w/w) ratio, while a control group (without PBAT) was labeled as P-CK. Gas measurements were taken on the 1st, 4th, 7th, 10th, 14th, and 25th days following the addition of PBAT, with the monitoring and sampling following a fixed sequence.

The CH₄/CO₂ measurements using FTIR spectroscopy

The schematic diagram of the experiment setup is shown in Fig. 1b. The FTIR spectrometer used was the Bruker V70 (Bruker, Karlsruhe, Germany). For details on the spectrometer's specifications, performance, and calibration procedures, refer to our previous study[14]. In this work, a long optical-path gas cell (20 m, Pike Technologies, Fitchburg, United States) installed on the FTIR spectrometer was connected to a static chamber via the plastic gas tube, with gas circulation driven by a mini gas pump.

At the 5th, 10th, and 15th minutes after placing the soil sample into the static chamber, the gas pump was turned on to ensure full gas circulation and to measure spectra. Data acquisition was performed using the spectrometer's accompanying software. After each measurement, the air in the static chamber and gas cell was refreshed to ensure a clean background, and three replicate experiments were conducted. Gas molecules exhibit specific absorption in different infrared wavelengths, which can be used for both quantitative and qualitative analysis. The identification of CH₄/CO₂ absorption peaks in the FTIR spectra was based on measurements taken on the first day and compared with the standard CH₄ absorption spectra in the National Institute of Standards and Technology (NIST) database[23].

Exploration of the CH₄ quantification method based on FTIR spectroscopy

The Beer-Lambert Law forms the foundation of FTIR spectroscopy theory[24], as shown in Eq. (1).

$$A = \varepsilon \cdot l \cdot c \tag{1}$$

Where A represents absorbance, ε (cm²·mol⁻¹) is the molar absorption coefficient, l (cm) is the optical path length, and c (mol·cm⁻³) is the concentration. ε, an intrinsic property of the gas indicating the absorption capacity per unit concentration, is obtained by multiplying the single molecule absorption coefficient, Ka (cm²·molecule⁻¹), by Avogadro's number (6.023×10²³ molecules·mol⁻¹). Ka corresponding to different wavenumbers at experimental temperatures can be sourced from the High-Resolution Transmission Molecular Absorption Database (HITRAN)[25]. Based on this information, we can convert the absorbance measured at the main absorbance peak into concentration values expressed in mol·cm⁻³. Considering the system's volume (fully accounting for the geometric volumes of the gas cell, static chamber, gas tubing, and the samples) and molar mass, we further determine target gas mass in the circulation system. Lastly, the flux is calculated based on the change in its mass over time, expressed in mg·m²·h⁻¹.

We validated the results by collecting gas and performing GC analysis (Fig. 1c). Briefly, the glass cylinder was tightly sealed with a preservative film for 5 min to equilibrate the headspace. Then, 30 mL of headspace gas was withdrawn using a gas-tight syringe and transferred into a 12 mL evacuated glass vial, marked as vial-1. After another 5 min, the process was repeated to fill a second vial, vial-2. The CH₄ concentrations in these samples were determined with a GC system (Agilent 7890–0468, California, USA) equipped with a flame ionization detector and electron capture detector. The GC was calibrated with standard gas after every twelve samples. Finally, the measured concentration data were converted into fluxes over time.

The soil sample analysis using ATR-FTIR spectroscopy

After the incubation experiments concluded, we destructively sampled and dried the soil samples. We used an ATR accessory, the GladiATR Illuminate model (Pike Technologies, Fitchburg, United States), fitted onto the FTIR spectrometer. For specific ATR measurement methods, please refer to our prior work[15]. In this study, we conducted three measurements each on the dried P-CK, P-PBAT samples, and BPs-PBAT (Fig. 1d).

Statistical analysis

Spectral data collection, preprocessing, peak identification, and area calculation were all conducted in OPUS 6.5 software (Bruker, Karlsruhe, Germany). The correlation analysis of the acquired data and the creation of graphs were performed using Origin 2023b (OriginLab Corporation, Northampton, United States).

Results and discussion

Identification of CH₄ and CO₂ absorption peaks

The infrared absorption spectra of gases emitted from P-CK are depicted in Fig. 2. Among them, CH₄ standards from the NIST database, measured at 4 cm⁻¹ resolution, were used for comparison[23]. Our experiments, conducted
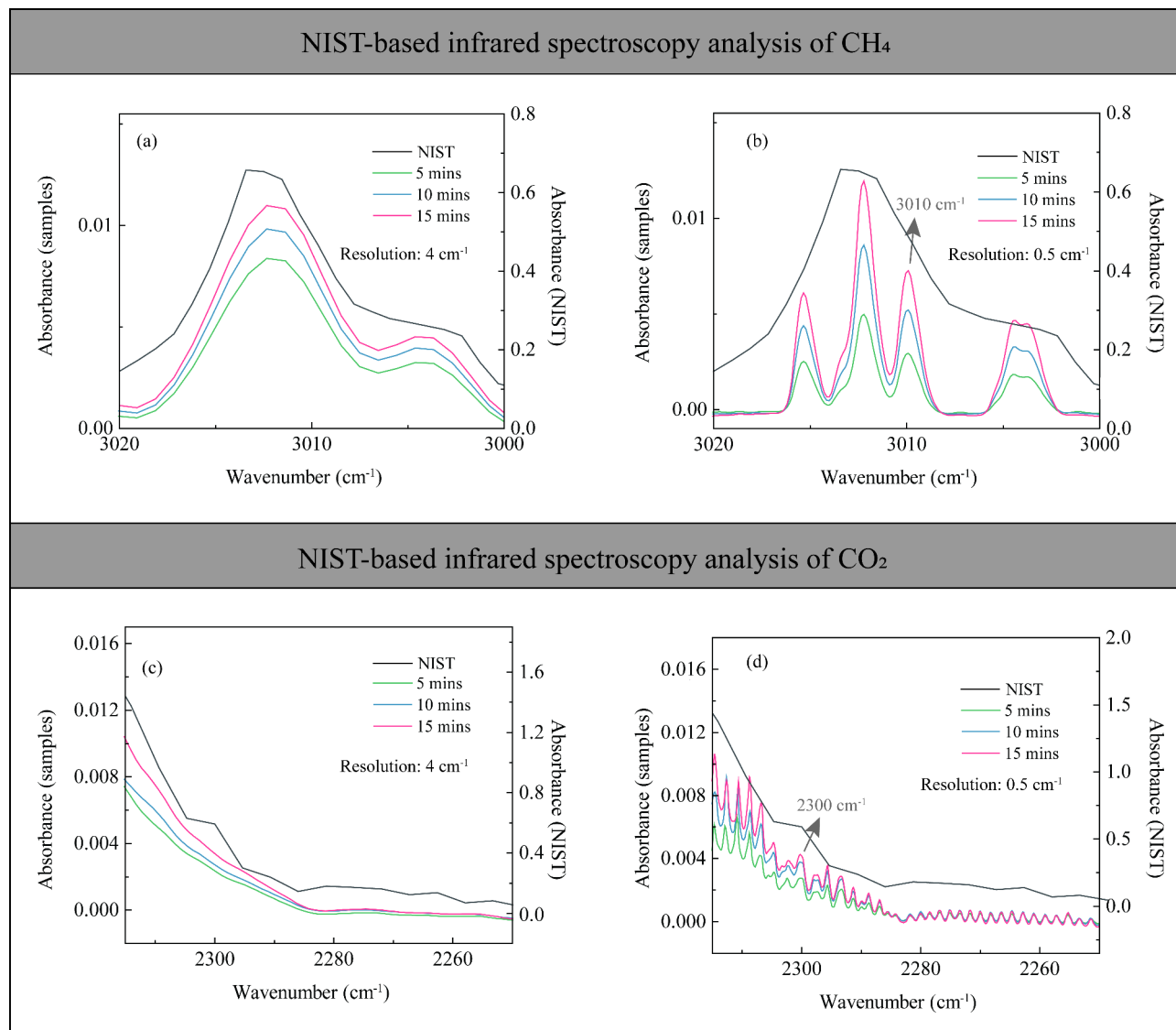
Fig. 2. The FTIR spectra of the volatiles released from P-CK. In the 3020 to 3000 cm^{-1} range, the infrared spectra obtained at resolutions of 4 cm^{-1} (**a**) and 0.5 cm^{-1} (**b**) are compared with CH$_4$ spectra from the NIST database. The spectra ranging from 2315 to 2250 cm^{-1} are compared with CO$_2$ spectra from the NIST database, as shown in (**c**) and (**d**).

at the same resolution, yielded spectra nearly identical in absorbance, indicating accurate measurement of soil-volatilized CH$_4$ (Fig. 1a). The 3020 to 3000 cm^{-1} band represents the typical CH$_4$ absorption peaks[26]. However, the lower resolution failed to discern specific absorption peaks, so we switched to a resolution of 0.5 cm^{-1}, successfully identifying four peaks (Fig. 1b). The 3010 cm^{-1} peak, frequently used by researchers for CH$_4$ identification and quantification, demonstrated an absorbance gradient over measurement time[27–29].

For CO$_2$, the 2315 to 2260 cm^{-1} range includes a subordinate peak of the infrared absorption (Fig. 2c and d). Although the main peak at 2349 cm^{-1} was saturated and unusable in our experiments, this spectral range still reflected CO$_2$ concentration changes. Researchers can study CO$_2$ using the absorption peak around 2300 cm^{-1} frequently[30,31]. These results show the success of our method in measuring temporal changes in soil-volatilized CH$_4$/CO$_2$.

Soil CH$_4$/CO$_2$ emissions

The CH$_4$/CO$_2$ emissions from paddy soil were significantly influenced by the introduction of PBAT. Figure 3 compared to the infrared spectral data of P-CK and P-PBAT on the 1st day. Within 5 min, the absorbance at 3010 cm^{-1} for P-PBAT was about 3% higher than that of P-CK, and at 2300 cm^{-1}, it was approximately 3.1 times that of P-CK.

Throughout the incubation period, CH$_4$ and CO$_2$ showed a pronounced response to PBAT. Based on CH$_4$ peaks at 3010 cm^{-1} and CO$_2$ peaks at 2300 cm^{-1}, we analyzed the absorbance increment within 5 to 10 min to study the emission patterns of CH$_4$ and CO$_2$ (Fig. 4). The emission rates of CH$_4$ and CO$_2$ from the soil both showed a trend
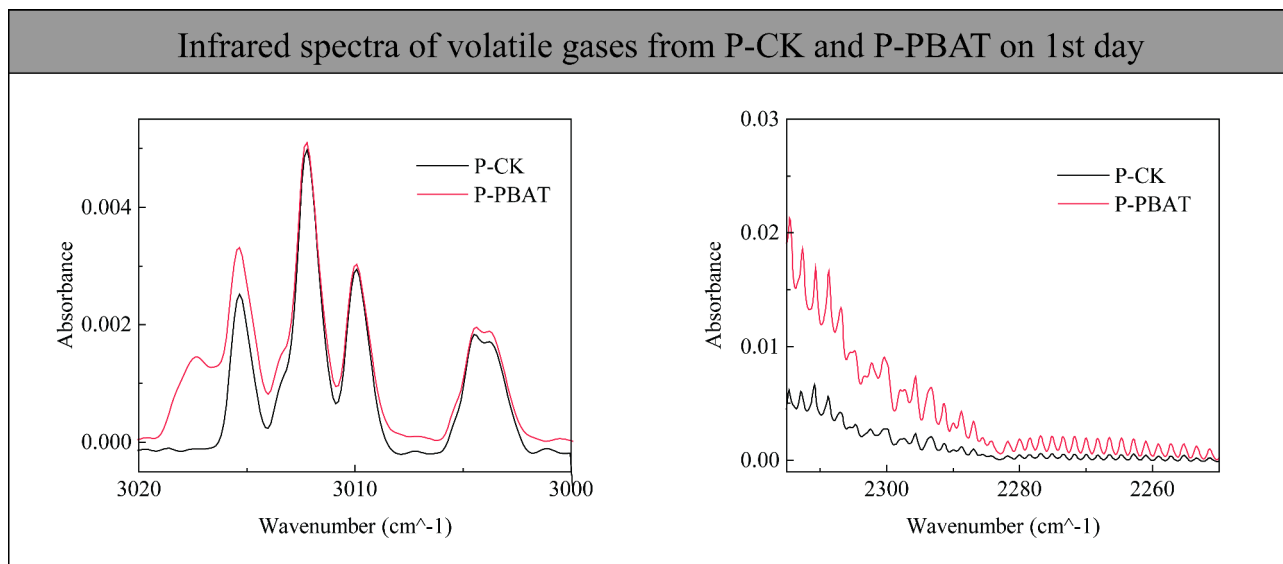
Fig. 3. The impact of PBAT on soil FTIR spectra. (**a**) Infrared absorption peaks within the 3020 to 3000 cm^{-1} (**a**) and the 2315 to 2250 cm^{-1} (**b**).

of increasing initially and then decreasing. Throughout the experimental period, the CH$_4$ emissions from the P-PBAT were consistently higher than those from the P-CK, with the peak emissions occurring on the seventh day. The absorbance increments for P-CK and P-PBAT were 0.005 and 0.46, respectively, a difference of 92 times (Fig. 4a and b), indicating that PBAT significantly promoted methane emissions from the soil. The same effect is also reflected in the CO$_2$ emission analysis results, where the peak CO$_2$ emission absorbance increments for P-CK and P-PBAT were 0.0023 and 0.49, respectively (Fig. 4c and d). This significant increase suggests complex interactions between Bio-MPs and the soil microbial community, enhancing soil GHG release, consistent with previous studies[32,33]. It is worth noting that the temperature during the experiment was about 10°C, which could also affect microbial activity and gas emission. Because temperature directly affects microbial activity and decomposition rates, warmer temperatures generally increase microbial metabolism, leading to higher emissions of CH$_4$ and CO$_2$, especially in environments like wetlands where anaerobic conditions prevail[34]. Further analysis of the relationship between absorbance increment at the two wavelengths revealed a Pearson's r of 0.48 (Fig. 4e), indicating a moderate correlation between soil-emitted CH$_4$/CO$_2$.

In general, the impacts of PBAT can be attributed to its metabolic pathways, degradation dynamics, and specific interactions with soil microbes[35]. The impact may stem from the degradation process itself, as well as from the increased activity of soil microorganisms promoted by the degradation process[36–38], highlighting the need for in-depth research on the complex effects and mechanisms of Bio-MPs on soil GHG emissions.

Exploration of CH$_4$ quantitative method based on FTIR spectroscopy

In our study, the absorbance at 3010 cm^{-1} was utilized for quantifying CH$_4$ concentrations. However, the 2300 cm^{-1} peak, not being a common peak for quantifying CO$_2$ concentrations, might be influenced by other gases and was only suitable for qualitative analysis of CO$_2$ concentration changes[27,30]. Therefore, we compared the measurement results based on FTIR spectroscopy and GC. We converted the absorbance data at 3010 cm^{-1} into CH$_4$ concentration data based on infrared spectroscopy theory and calculated the flux and cumulative emissions (Fig. 5). The quantification results exhibited trends similar to those observed in gas chromatography analysis. The Pearson correlation coefficient between the two datasets was 0.98, and the mean squared error was 1.67, indicating no significant statistical difference between them. However, the numerical discrepancy between the datasets may be attributed to factors such as system errors, cross-interference from water vapor, and environmental influences on the parameters used for quantitative calculations[39,40]. In conclusion, while the numerical deviation between the two datasets is explainable, the trends demonstrate a high degree of consistency.

The CH$_4$ emission flux from P-CK on the 7th day was 5.4 mg·m^2·h^{-1} (Fig. 5a), aligning closely with previous findings[41]. For P-PBAT, the flux dramatically increased to 587 mg·m^2·h^{-1} (Fig. 5b), with cumulative emissions during the experimental period being 42 times that of P-CK (Fig. 5c). This significant enhancement is consistent with earlier research[32]. Emission fluxes are influenced by a combination of soil properties and environmental factors, and the observed results represent the overall performance after a dynamic balance of multiple influencing factors. Future efforts will focus on refining FTIR quantitative analysis by minimizing interferences, building on these initial but significant findings.

ATR spectrum of soil

The ATR spectra of three samples (P-CK, P-PBAT, Bio-MPs-PBAT) are shown in Fig. 6a. In the wavenumber ranges of 3530–3525 cm^{-1} and 3266–3218 cm^{-1}, the ATR spectra of P-CK exhibit noticeable differences from P-PBAT and Bio-MPs-PBAT. The Principal component analysis (PCA) of the ATR spectra for P-CK and
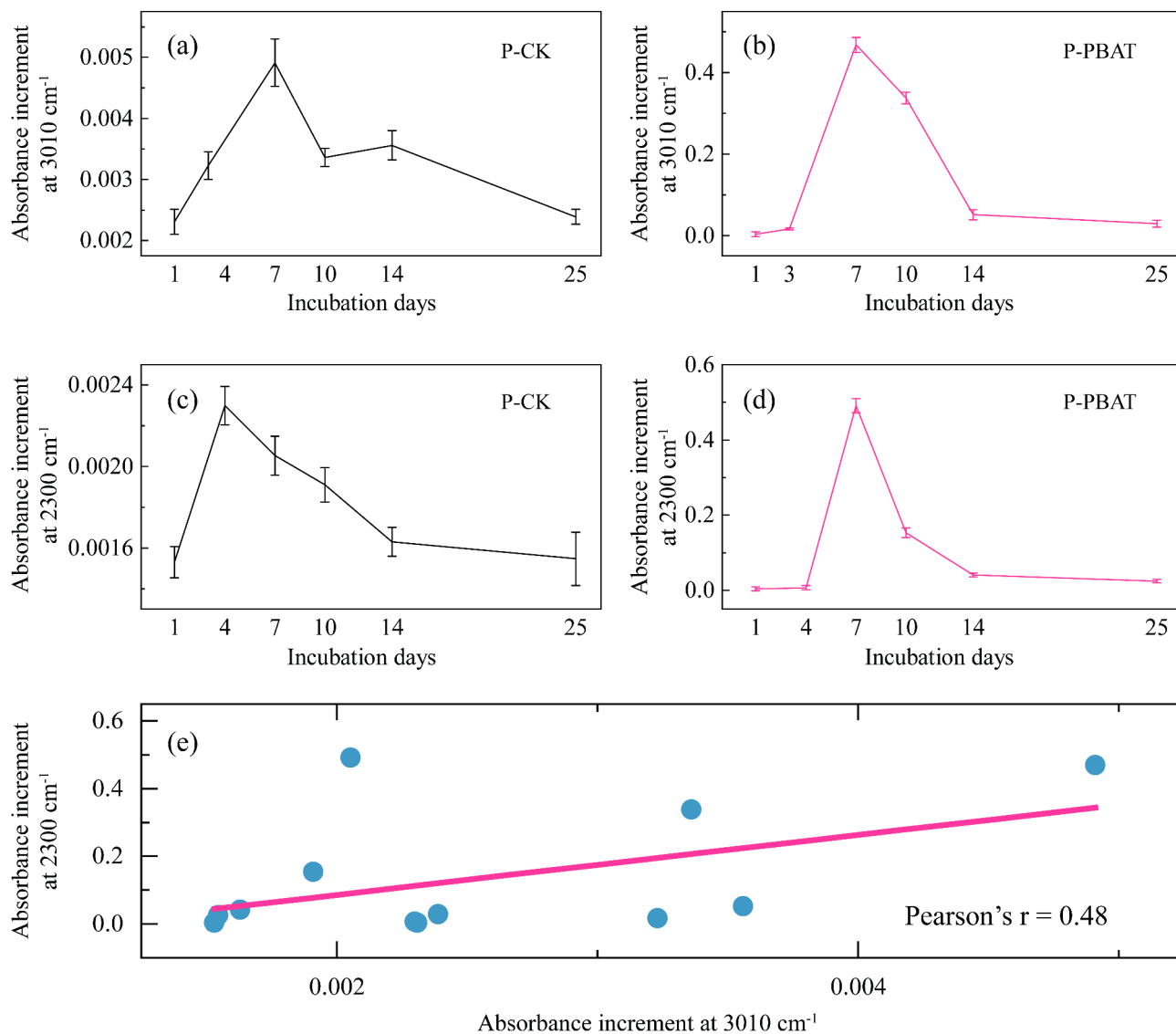
Fig. 4. Infrared spectroscopic analysis of volatiles from P-CK and P-PBAT during incubation. Absorbance increments at 3010 cm^{-1} and 2300 cm^{-1} (**a–d**) and the correlation between them (**e**).
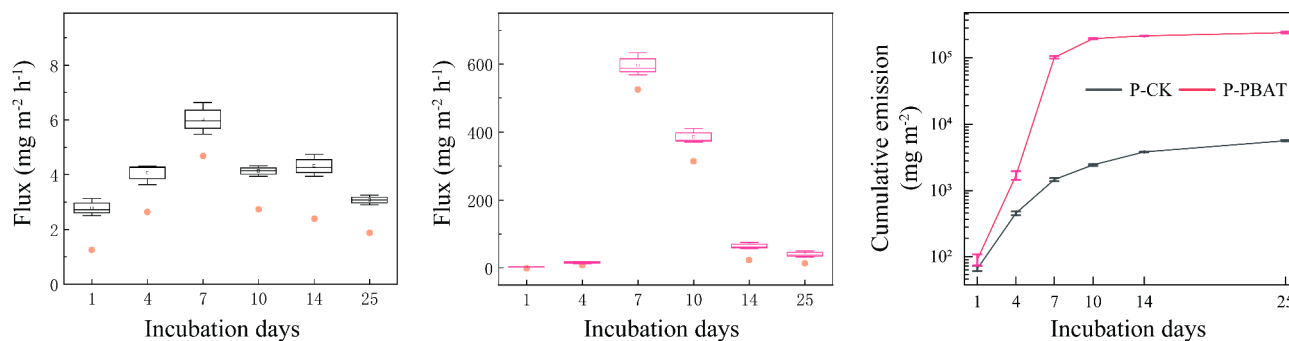

Fig. 5. Quantitative results of CH$_4$ Flux Based on FTIR Spectroscopy. CH$_4$ emission fluxes of P-CK (**a**) and P-PBAT (**b**) and the cumulative CH$_4$ emissions over the incubation period (**c**). Orange dots indicate results measured by GC.
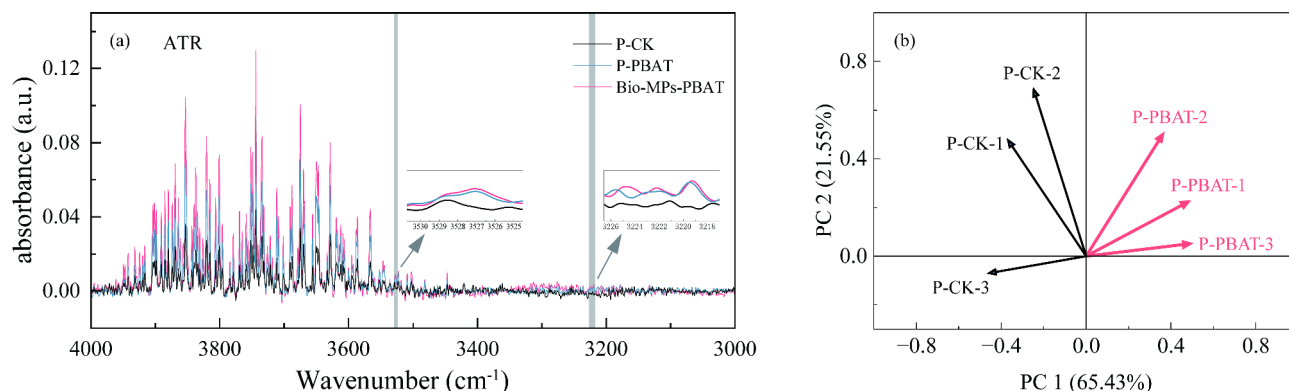
Fig. 6. ATR-FTIR analysis of soil samples. (**a**) ATR spectra of P-CK, P-PBAT, and Bio-MPs-PBAT. (**b**) PCA analysis of ATR spectral data.

P-PBAT shows that the two spectral data sets can be distinctly separated (Fig. 6b). This indicates that ATR spectroscopy, a straightforward method for identifying solid surface structures[42], has the potential to determine soil contamination by PBAT.

Conclusion

Our findings highlight the potential of using FTIR spectroscopy to continuously monitor soil CH_4/CO_2. Additionally, we have elucidated the relationship between Bio-MPs-PBAT and soil GHG emissions. BPs can reduce the accumulation of plastic waste in the environment. However, their degradation process may generate GHGs or indirectly intensify the greenhouse effect by promoting microbial activity. Despite these concerns, compared to traditional plastics, BPs can reduce plastic pollution and are relatively more environmentally friendly. These studies contribute to facilitating the establishment of more accurate models and effective strategies to mitigate the potential impact of Bio-MPs on soil ecosystems. Nevertheless, our study has certain limitations, including constraints associated with laboratory-scale monitoring and the need for further investigation into the underlying mechanisms. Although we validated the feasibility of the FTIR system in monitoring greenhouse gas emissions through gas chromatography analysis with synchronized sampling, additional online measurement techniques, such as TDLAS, are required to further verify the system's reliability. Moreover, exploratory CH_4 quantitative methods require further research. Future work should address these limitations and focus on developing compact FTIR monitoring systems for real-time field measurements. Additionally, the broader application of FTIR spectroscopy in the field of soil greenhouse gas emissions should be explored.

Data availability

The datasets used and/or analyzed during the current study are available from the corresponding author on reasonable request.

References

1. Netz, B., Davidson, O., Bosch, P., Dave, R. & Meyer, L. Climate change Climate change 2007: Mitigation. Contribution of working group III to the fourth assessment report of the intergovernmental panel on climate change. *Intergovernmental Panel on Climate Change*. https://scholar.google.com/scholar?cluster=6951778826326079882&hl=zh-CN&as_sdt=2005&sciodt=0,5 (2017)
2. Shukla, P. R. *et al.* Climate Change and Land: An IPCC special report on climate change, desertification, land degradation, sustainable land management, food security, and greenhouse gas fluxes in terrestrial ecosystems. *Intergovernmental Panel on Climate Change*. https://scholar.google.com/scholar?cluster=5624169081115207143&hl=zh-CN&as_sdt=2005&sciodt=0,5 (2019).
3. Kabir, A. H. M. E. et al. Assessing small-scale freshwater microplastics pollution, land-use, source-to-sink conduits, and pollution risks: Perspectives from Japanese rivers polluted with microplastics. *Sci. Total Environ.* **768**, 144655. https://doi.org/10.1016/j.scitotenv.2020.144655 (2021).
4. Petersen, F. & Hubbart, J. A. The occurrence and transport of microplastics: The state of the science. *Sci. Total Environ.* **758**, 143936. https://doi.org/10.1016/j.scitotenv.2020.143936 (2021).
5. Wang, C. et al. Biodegradable microplastics (BMPs): A new cause for concern?. *Environ. Sci. Pollut. Res.* **28**, 66511–66518. https://doi.org/10.1007/s11356-021-16435-4 (2021).
6. Sun, Y. et al. Biodegradable microplastics enhance soil microbial network complexity and ecological stochasticity. *J. Hazard. Mater.* **439**, 129610. https://doi.org/10.1016/j.jhazmat.2022.129610 (2022).
7. Qin, M. et al. A review of biodegradable plastics to biodegradable microplastics: Another ecological threat to soil environments?. *J. Clean. Prod.* **312**, 127816. https://doi.org/10.1016/j.jclepro.2021.127816 (2021).
8. Fan, P., Yu, H., Xi, B. & Tan, W. A review on the occurrence and influence of biodegradable microplastics in soil ecosystems: Are biodegradable plastics substitute or threat?. *Environ. Int.* **163**, 107244. https://doi.org/10.1016/j.envint.2022.107244 (2022).
9. Wachiye, S. et al. Soil greenhouse gas emissions under different land-use types in savanna ecosystems of Kenya. *Biogeosciences* **17**, 2149–2167. https://doi.org/10.5194/bg-17-2149-2020 (2020).

10. Ye, X. et al. Impacts of irrigation methods on greenhouse gas emissions/absorptions from vegetable soils. *J. Soils Sediments* **20**, 723–733. https://doi.org/10.1007/s11368-019-02422-3 (2020).
11. Schindler, T. et al. Short-term flooding increases CH_4 and N_2O emissions from trees in a riparian forest soil-stem continuum. *Sci. Rep.* **10**, 3204. https://doi.org/10.1038/s41598-020-60058-7 (2020).
12. Picó, Y. & Barceló, D. Pyrolysis gas chromatography-mass spectrometry in environmental analysis: Focus on organic matter and microplastics. *Trends Analyt. Chem.* **130**, 115964. https://doi.org/10.1016/j.trac.2020.115964 (2020).
13. Stockwell, C. E. *et al.* Trace gas emissions from combustion of peat, crop residue, domestic biofuels, grasses, and other fuels: Configuration and Fourier transform infrared (FTIR) component of the fourth Fire Lab at Missoula Experiment (FLAME-4). *Atmos. Chem. Phys.* **14**, 9727-9754. https://doi.org/10.5194/acp-14-9727-2014 (2014).
14. Dong, D., Jiao, L., Li, C. & Zhao, C. Rapid and real-time analysis of volatile compounds released from food using infrared and laser spectroscopy. *Trends Analyt. Chem.* **110**, 410–416. https://doi.org/10.1016/j.trac.2018.11.039 (2019).
15. Chen, C., Dong, D., Li, Z. & Wang, X. A novel soil nutrient detection method based on combined ATR and DRIFT mid-infrared spectra. *Anal. Methods* **9**, 528–533. https://doi.org/10.1039/C6AY02904C (2017).
16. Jiao, L., Dong, D., Han, P., Zhao, X. & Du, X. Identification of the mango maturity level by the analysis of volatiles based on long optical-path FTIR spectroscopy and a molecular sieve. *Anal. Methods* **9**, 2458–2463. https://doi.org/10.1039/C7AY00149E (2017).
17. Mansa, R. & Zou, S. Thermogravimetric analysis of microplastics: A mini review. *Environ. Adv.* **5**, 100117. https://doi.org/10.1016/j.envadv.2021.100117 (2021).
18. Li, F. et al. Identification and visualization of environmental microplastics by Raman imaging based on hyperspectral unmixing coupled machine learning. *J. Hazard. Mater.* **465**, 133336. https://doi.org/10.1016/j.jhazmat.2023.133336 (2024).
19. Xu, X. et al. Detection of soil organic matter from laser-induced breakdown spectroscopy (LIBS) and mid-infrared spectroscopy (FTIR-ATR) coupled with multivariate techniques. *Geoderma* **355**, 113905. https://doi.org/10.1016/j.geoderma.2019.113905 (2019).
20. Xing, Z., Du, C., Shen, Y., Ma, F. & Zhou, J. A method combining FTIR-ATR and Raman spectroscopy to determine soil organic matter: Improvement of prediction accuracy using competitive adaptive reweighted sampling (CARS). *Comput. Electron. Agric.* **191**, 106549. https://doi.org/10.1016/j.compag.2021.106549 (2021).
21. Brockhaus, S., Petersen, M. & Kersten, W. A crossroads for bioplastics: exploring product developers' challenges to move beyond petroleum-based plastics. *J. Clean. Prod.* **127**, 84–95. https://doi.org/10.1016/j.jclepro.2016.04.003 (2016).
22. Gong, W. et al. Comparative analysis on the sorption kinetics and isotherms of fipronil on nondegradable and biodegradable microplastics. *Environ. Pollut.* **254**, 112927. https://doi.org/10.1016/j.envpol.2019.07.095 (2019).
23. Zhang, L., Liu, C. & Li, Q. Molecular simulations of competitive adsorption behavior between CH_4-C_2H_6 in K-illite clay at supercritical conditions. *Fuel* **260**, 116358. https://doi.org/10.1016/j.fuel.2019.116358 (2020).
24. Mayerhöfer, T. G., Pahlow, S. & Popp, J. The Bouguer-Beer-Lambert law: Shining light on the obscure. *ChemPhysChem* **21**, 2029–2046. https://doi.org/10.1002/cphc.202000464 (2020).
25. Stolarczyk, N. et al. Evaluation of different parameterizations of temperature dependences of the line-shape parameters based on ab initio calculations: Case study for the HITRAN database. *J. Quant. Spectrosc. Radiat. Transfer* **240**, 106676. https://doi.org/10.1016/j.jqsrt.2019.106676 (2020).
26. Kazanskii, V. B., Serykh, A. I. & Bell, A. T. Diffuse-Reflectance IR Spectra of Methane Adsorbed on NaZSM-5 and HZSM-5 Zeolites. *Kinet. Catal.* **43**, 419–426. https://https://doi.org/10.1023/A:1016022305076 (2002).
27. Wilcox, E. M., Roberts, G. W. & Spivey, J. J. Direct catalytic formation of acetic acid from CO_2 and methane. *Catal. Today* **88**, 83–90. https://doi.org/10.1016/j.cattod.2003.08.007 (2003).
28. Hirschmann, C. B., Uotila, J., Ojala, S., Tenhunen, J. & Keiski, R. L. Fourier transform infrared photoacoustic multicomponent gas spectroscopy with optical cantilever detection. *Appl. Spectrosc.* **64**, 293–297. https://doi.org/10.1366/000370210790918490 (2010).
29. Geminale, A., Formisano, V. & Giuranna, M. Methane in Martian atmosphere: Average spatial, diurnal, and seasonal behaviour. *Planet. Space Sci.* **56**, 1194–1203. https://doi.org/10.1016/j.pss.2008.03.004 (2008).
30. Coenen, K., Gallucci, F., Mezari, B., Hensen, E. & van Sint Annaland, M. An in-situ IR study on the adsorption of CO_2 and H_2O on hydrotalcites. *J. CO_2 Util.* **24**, 228–239. https://doi.org/10.1016/j.jcou.2018.01.008 (2018).
31. Matricardi, M. Technical note: An assessment of the accuracy of the RTTOV fast radiative transfer model using IASI data. *Atmos. Chem. Phys.* **9**, 6899-6913, https://doi.org/10.5194/acp-9-6899-2009 (2009).
32. Rauscher, A. et al. Biodegradable microplastic increases CO_2 emission and alters microbial biomass and bacterial community composition in different soil types. *Appl. Soil Ecol* **182**, 104714. https://doi.org/10.1016/j.apsoil.2022.104714 (2023).
33. Fan, M., Rakotondrabe, T. F., Chen, G. & Guo, M. Advances in microbial analysis: Based on volatile organic compounds of microorganisms in food. *Food Chem.* **418**, 135950. https://doi.org/10.1016/j.foodchem.2023.135950 (2023).
34. Zhong, X., Qi, J., Li, H., Dong, L. & Gao, D. Seasonal distribution of microbial activity in bioaerosols in the outdoor environment of the Qingdao coastal region. *Atmos. Environ.* **140**, 506–513. https://doi.org/10.1016/j.atmosenv.2016.06.034 (2016).
35. Li, L., Geng, S., Li, Z. & Song, K. Effect of microplastic on anaerobic digestion of wasted activated sludge. *Chemosphere* **247**, 125874. https://doi.org/10.1016/j.chemosphere.2020.125874 (2020).
36. Sun, Y. et al. Biodegradable and conventional microplastics exhibit distinct microbiome, functionality, and metabolome changes in soil. *J. Hazard. Mater.* **424**, 127282. https://doi.org/10.1016/j.jhazmat.2021.127282 (2022).
37. Fei, Y. et al. Response of soil enzyme activities and bacterial communities to the accumulation of microplastics in an acid cropped soil. *Sci. Total Environ.* **707**, 135634. https://doi.org/10.1016/j.scitotenv.2019.135634 (2020).
38. Ji, M. et al. Different microplastics in anaerobic paddy soils: Altering methane emissions by influencing organic matter composition and microbial metabolic pathways. *Chem. Eng. J.* **469**, 144003. https://doi.org/10.1016/j.cej.2023.144003 (2023).
39. Lin, C. H., Grant, R. H., Heber, A. J. & Johnston, C. T. Application of open-path Fourier transform infrared spectroscopy (OP-FTIR) to measure greenhouse gas concentrations from agricultural fields. *Atmos. Meas. Tech.* **12**, 3403–3415. https://doi.org/10.5194/amt-12-3403-2019 (2019).
40. Zhao, Y. et al. A novel strategy for large-scale metabolomics study by calibrating gross and systematic errors in gas chromatography-mass spectrometry. *Anal. Chem.* **88**, 2234–2242. https://doi.org/10.1021/acs.analchem.5b03912 (2016).
41. Miyata, A., Leuning, R., Denmead, O. T., Kim, J. & Harazono, Y. Carbon dioxide and methane fluxes from an intermittently flooded paddy field. *Agric. For. Meteorol.* **102**, 287–303. https://doi.org/10.1016/S0168-1923(00)00092-7 (2000).
42. Koçak, A., Wyatt, W. & Comanescu, M. A. Comparative study of ATR and DRIFT infrared spectroscopy techniques in the analysis of soil samples. *Forensic Sci. Int.* **328**, 111002. https://doi.org/10.1016/j.forsciint.2021.111002 (2021).

Acknowledgements

Author contributions

Y.H., W.G., and D.D. conceived the idea. Y.H., and D.D. designed the experiments. L.J., C.Z., W.D., and D.D. participated in the data presentation, analysis, and discussion. Y.H. wrote the final manuscript draft. All authors reviewed the manuscript draft and approved the publication of the manuscript.

Declarations

Competing interests
The authors declare no competing interests.

Additional information
Correspondence and requests for materials should be addressed to W.G. or D.D.

Reprints and permissions information is available at www.nature.com/reprints.

Publisher's note Springer Nature remains neutral with regard to jurisdictional claims in published maps and institutional affiliations.